ELSEVIER

Marine Geology 232 (2006) 227–235

MARINE GEOLOGY
INTERNATIONAL JOURNAL OF MARINE GEOLOGY, GEOCHEMISTRY AND GEOPHYSICS

www.elsevier.com/locate/margeo

High-resolution benthic foraminifer $\delta^{13}C$ records in the South China Sea during the last 150 ka

Gang-Jian Wei [a,b,*], Chi-Yue Huang [b,c], Chia-Chun Wang [b], Meng-Yan Lee [b], Kuo-Yen Wei [b]

[a] *Key Laboratory of Isotope Geochronology and Geochemistry, Guangzhou Institute of Geochemistry, Chinese Academy of Sciences, Guangzhou, Guangdong 510640, China*
[b] *National Taiwan University, Taipei, Taiwan*
[c] *National Cheng Kung University, Tainan, Taiwan*

Received 19 May 2005; received in revised form 16 July 2006; accepted 2 August 2006

Abstract

High-resolution $\delta^{13}C$ ratios of benthic foraminifer, *Cibicidoides wuellerstorfi*, in Core MD97-2151 from the southern South China Sea (SCS) and Core SO50-31KL from the northern SCS indicate deep-water variations in the SCS during the last 150 ka. The $\delta^{13}C$ records of both show a general variation pattern with higher $\delta^{13}C$ during interglacial periods than glacial periods, and rapid increases during terminations. This variation pattern resembles those of the West Pacific intermediate/deep water, the sources of the SCS deep water and the general variation of global deep water, indicating that the variation of the SCS deep water is largely controlled by global factors, such as carbon cycles and global deep-water circulation. Spectra analysis exhibits robust Milankovitch cycles in the SCS deep-water $\delta^{13}C$, again supporting global controls. Significant semi-precession cycles can also be seen in the spectra, implying that changes of local surface productivity also influence the SCS deep-water $\delta^{13}C$.

Keywords: carbon isotopes; benthic foraminifer; deep-water ventilation; South China Sea

1. Introduction

The $\delta^{13}C$ values of the dissolved inorganic carbon (DIC) in deep-water is one of the best tracers for deep-water circulation (Curry and Lohmann, 1982; Shackleton et al., 1983; Duplessy et al., 1984; Duplessy and Shackleton, 1985; Boyle and Keigwin, 1985/86). When deep-water flows, organic matter with more negative $\delta^{13}C$ sinks from surface water and decomposes, resulting in decreases of DIC $\delta^{13}C$. The $\delta^{13}C$ of benthic foraminifer, *Cibicidoides wuellerstorfi* are very close to the dissolved CO_2 of deep-water, thus can well proxy deep-water $\delta^{13}C$ (Belanger et al., 1981; Duplessy et al., 1984; Curry et al., 1988). Moreover, the relationship between the $\delta^{13}C$ of *C. wuellerstorfi* and DIC is quite robust, and does not change with water depth (McCorkle and Keigwin, 1994). Therefore, the $\delta^{13}C$ values of *C. wuellerstorfi* represent deep-water $\delta^{13}C$ (Keigwin, 1998), and are generally used to reconstruct deep-water variations.

* Corresponding author. Key Laboratory of Isotope Geochronology and Geochemistry, Guangzhou Institute of Geochemistry, Chinese Academy of Sciences, Guangzhou, Guangdong 510640, China. Tel.: +86 20 85290093; fax: +86 20 59290130.
E-mail address: gjwei@gig.ac.cn (G.-J. Wei).

0025-3227/$ - see front matter © 2006 Elsevier B.V. All rights reserved.
doi:10.1016/j.margeo.2006.08.005

The South China Sea is the largest marginal sea in the west Pacific with several connections to the Pacific and Indian Ocean. The Bashi Strait, located in the northeast SCS with a sill depth of about 2500 m, is the only gateway that enables deep water to flow into the SCS from the west Pacific (Chao et al., 1996). At present, deep water from West Philippine Sea flows into the SCS through this gateway and fills the abyssal SCS from north to south (Wang, 1986). Two deep upwelling systems off southwest Taiwan and Vietnam help to renew the SCS deep water (Chao et al., 1996). Paleoceanographic studies indicate that both the intermediate water mass (IWM) and deep-water mass (DWM) above 2500 m in the west Pacific contribute to the deep-water of the SCS (Jian and Wang, 1997), and the ventilation of SCS deep-water is closely related to that in their sources (Jian and Wang, 1997). Because both the carbonate content in sediments and the sedimentary rates are low in the west Pacific, well-preserved high-resolution deep-water records are very rare. Therefore, records from the SCS are particularly valuable to understand the deep-water variations of the west Pacific (Jian and Wang, 1997).

Studies of deep-water ventilation in the SCS, based on benthic foraminifers, were carried out by Oppo and Fairbanks (1987), Winn et al. (1992), Miao and Thunell (1996), Jian and Wang (1997) and Jian et al. (1999, 2000). $\delta^{13}C$ values in benthic foraminifers were used to track deep-water variations (Oppo and Fairbanks, 1987; Winn et al., 1992; Jian and Wang, 1997; Wang et al., 1999). Previous studies showed that deep-water $\delta^{13}C$ in the SCS is generally lower than in the west Pacific (Winn

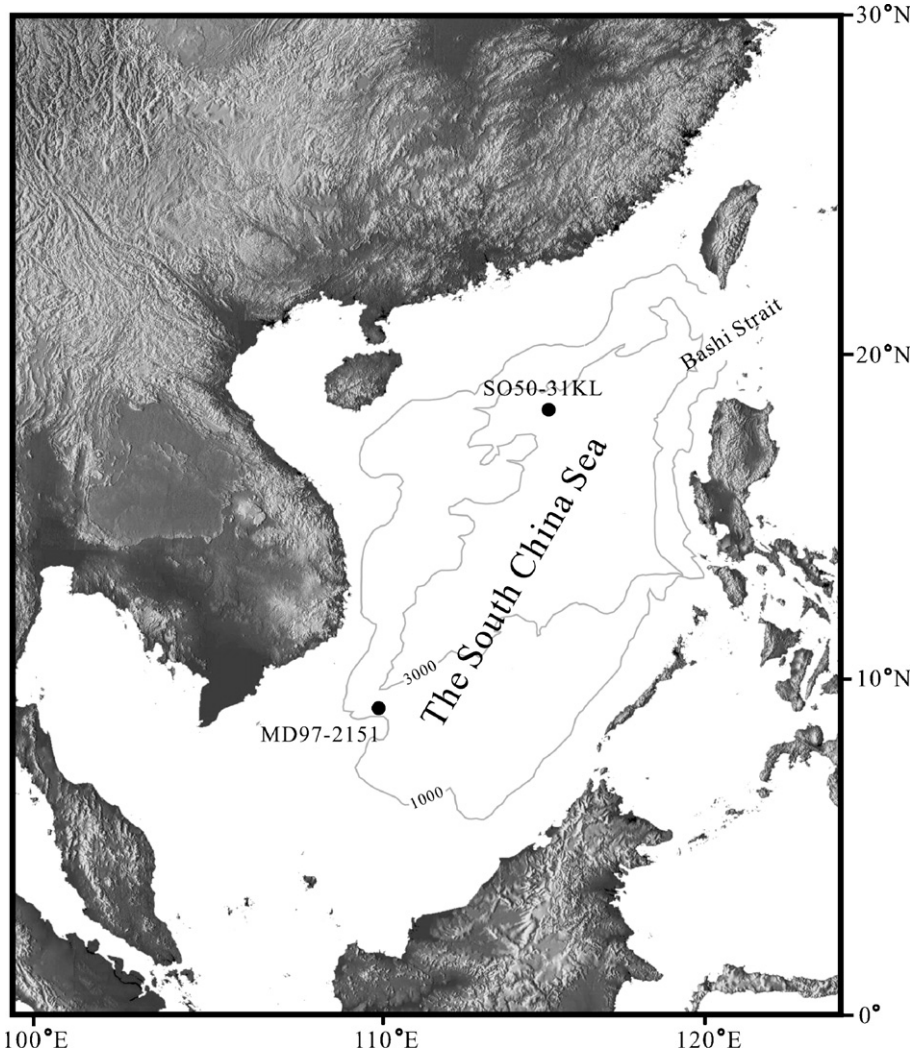

Fig. 1. Locations of Core MD97-2151 and Core SO50-31KL. Thin lines indicate the 1000 m and 3000 m isobaths.

et al., 1992), and benthic $\delta^{13}C$ in the southern SCS is generally more negative than in the northern SCS during glacials (Jian and Wang, 1997; Wang et al., 1999). High-resolution deep-water records in the SCS, however, are scarce, and deep-water variations are not well known. Moreover, spatial differences in organic matter fluxes from surface water are substantial in the SCS. Because higher organic fluxes provide more organic carbon to the deep water, the released carbon from decomposed organic matter may result in more negative $\delta^{13}C$ in deep water. Such spatial differences may result in abnormal deep-water $\delta^{13}C$ values (Wang et al., 1999), and obscure the deep-water ventilation signal in $\delta^{13}C$ records. Nonetheless, to what extent they influence deep-water $\delta^{13}C$ is not well known in the SCS.

We present two high-resolution benthic foraminiferal $\delta^{13}C$ records from the southern and northern SCS, which document deep-water variations during the last 150 ka. The northern record was obtained from sediment Core SO50-31KL, recovered at water depth of 3360 m, far below the sill depth of the Bashi Strait. The southern record was obtained from sediment Core MD97-2151, recovered at water depth of 1598 m, above the sill depth of the Bashi Strait. Comparisons of $\delta^{13}C$ in these two records and in records from other locations provide new insights into deep-water ventilation in the SCS within the last glacial/interglacial cycle.

2. Materials and methods

Sediment samples from Core SO50-31KL (18°45.4′N, 115°52.4′E, water depth 3360 m) and Core MD97-2151 (8°43.73′N, 109°52.17′E, water depth 1598 m) (Fig. 1) were used in this study. The recovered length was 2560 cm and 800 cm for Core MD97-2151 and Core SO50-31KL, respectively. Samples were taken every 4 cm in Core MD97-2151, and every 2 cm in Core SO50-31KL, corresponding to time resolution of about 0.2 kyr and 0.3 kyr for Core MD97-2151 and SO50-31KL, respectively. The benthic foraminifer, *C. wuellerstorfi*, was picked from the >150 μm size fraction of the samples for isotope analysis.

The foraminiferal tests were first ultrasonically washed in distilled water to remove adhering particles, and then soaked in 10% NaOCl solution for 24 h to remove organic materials. $\delta^{13}C$ and $\delta^{18}O$ were measured on a Finnegan MAT Delta Plus mass spectrometer coupled with a Kiel automatic carbonate device in the Department of Geology, National Taiwan University. On average, about 3 *C. wuellerstorfi* tests were measured for each sample. The oxygen and carbon isotopic ratios were calibrated to PDB standard via USGS standard NBS 19. Analysis on NBS 19 and a lab marble standard during this study provided an external precision of 0.08‰ and 0.05‰ for $\delta^{18}O$ and $\delta^{13}C$, respectively. About 50 samples from the two cores that had sufficient tests were double-checked, and the reproducibility is better than 0.08‰ and 0.05‰ for $\delta^{18}O$ and $\delta^{13}C$, respectively, which agreed with that of NBS 19 and the marble standard. The oxygen and carbon isotope results are presented in a Supplementary Data in the Appendix.

3. Age models

The age models for these two cores were initially generated from the $\delta^{18}O$ curve of the planktonic foraminifer *Globigerinoides sacculifer*, coupled with several AMS ^{14}C dates of planktonic foraminifers (Chen and Huang, 1998; Lee et al., 1999). Because of significant carbonate dissolution, the *G. sacculifer* tests in Core SO50-31KL were lack, resulting in relatively low resolution for the $\delta^{18}O$ curve (Chen and Huang, 1998). Here, we generated a new age model for Core SO50-31KL, based on the $\delta^{18}O$ curve of *C. wuellerstorfi* and the previous AMS ^{14}C ages. The age control points are listed in Table 1. In contrast to *G. sacculifer*, *C. wuellerstorfi* is more resistant to dissolution, and the resolution of the $\delta^{18}O$ curve of *C. wuellerstorfi* is higher, providing better age controls (Fig. 2).

We also established a new age model based on the $\delta^{18}O$ of *C. wuellerstorfi* for Core MD97-2151, although the resolution of the initial age model, based on

Table 1
Age control points for Core SO50-31KL

Depth (cm)	Age (ka)	Interpretation
5	0.924	C-14 [a]
35	6.045	C-14 [a]
41	7.441	C-14 [a]
87	12.05	MIS 2.0
161	17.85	MIS 2.2
233	24.11	MIS 3.0
293	28	MIS 3.1
399	43.88	MIS 3.13
450	50.21	MIS 3.3
541	55.45	MIS 3.31
576	58.96	MIS 4.0
609	64.09	MIS 4.22
651	73.91	MIS 5.0
700	79.25	MIS 5.1

MIS represents oxygen isotope events correlated to SPECMAP. Ages are from Martinson et al. (1987) except for MIS 3.1, which is from (Grootes et al., 1993).

[a] All calibrated to calendar years, data from Chen and Huang (1998).

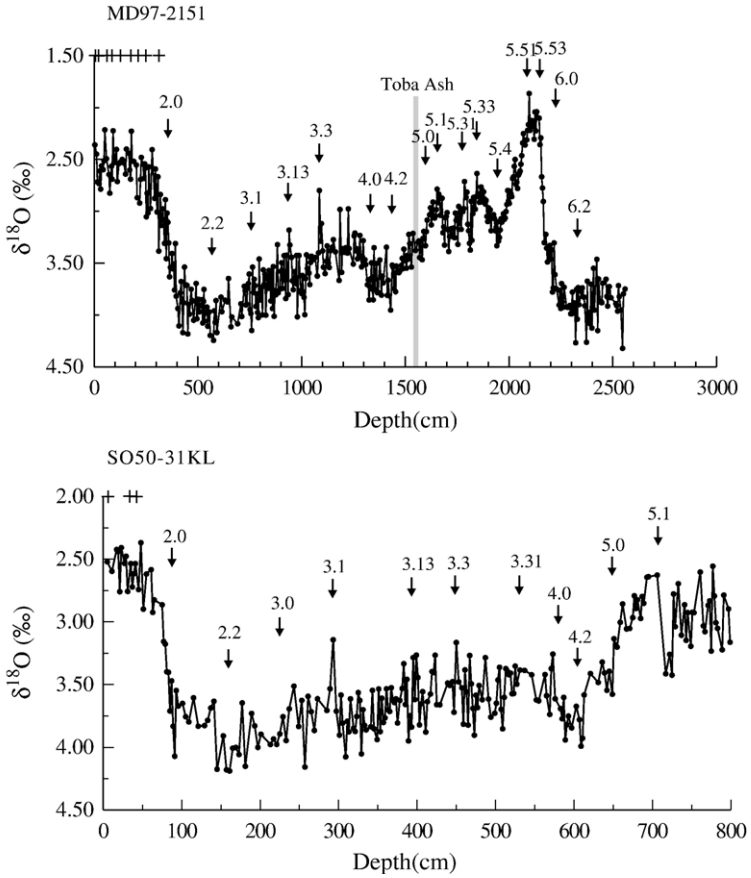

Fig. 2. Age correlation points for Core MD97-2151 (upper) and Core SO50-31KL (lower). Crosses indicate AMS ^{14}C dating points. Arrows indicate oxygen isotope events in comparison to SPECMAP. Shaded area indicates the Toba ash layer in Core MD97-2151.

G. sacculifer, is high enough. Because the δ^{18}O curve of *C. wuellerstorfi* follows more closely the SPECMAP than that of *G. sacculifer*, which exhibits nearly the same δ^{18}O at MIS 5.1, MIS 5.3 and MIS 5.5 (Lee et al., 1999), the new age model may provide better age controls. Previous AMS ^{14}C ages younger than 10 ka (Lee et al., 1999) and the volcanic glass layer at 1558 cm were used as additional age control points. This glass is considered to be related to the latest eruption of the Toba volcano in Sumatra at ~71 ka (Lee et al., 1999). The age control points are listed in Table 2 and the oxygen isotope curves for Core SO50-31KL and MD97-2151 are shown in Fig. 2.

The new age models for the two cores agree well with the former age models within errors of the SPECMAP ages (Martinson et al., 1987).

4. Carbon isotope results

The δ^{13}C curves of *C. wuellerstorfi* in Cores SO50-31KL and MD97-2151 are somehow similar both in variation patterns and values (Fig. 3). δ^{13}C is generally higher during interglacial periods than during glacial periods. The maximum δ^{13}C (about 0.2~0.3‰) in Core MD97-2151 occurs during Stage 1, and the minimum (about −0.9‰), showing an increasing trend towards the present since 150 ka (Fig. 3). Such trend is not so clear in Core SO50-31KL, where δ^{13}C values are similar during Stages 3 and 5, and during Stages 2 and 4. However, the maximum δ^{13}C (about 0.3‰) occurs during Stage 1, implying similar increasing trend towards the present like that in Core MD97-2151 (Fig. 3).

There are several negative spikes in the δ^{13}C curve of Core MD97-2151, centering at ~33 ka, ~38 ka and ~44 ka during Stage 3. The decreases in δ^{13}C are about −0.2‰ to −0.4‰, and lasted for less than 1000 years in general. Such negative peaks were not seen in Core SO50-31KL, although the resolution of the two cores is similar.

During Terminations I and II, δ^{13}C shows stepwise increases in both cores (Fig. 3). A positive δ^{13}C excursions with amplitude of about 0.1–0.15‰ in

Table 2
Age control points for Core MD97-2151

Depth (cm)	Age (ka)	Interpretation
3	0.938	C-14[a]
35	1.353	C-14[a]
71	2.143	C-14[a]
91	2.743	C-14[a]
127	3.697	C-14[a]
171	4.499	C-14[a]
211	5.648	C-14[a]
251	7.276	C-14[a]
311	9.927	C-14[a]
363.5	12.05	MIS 2.0
575.5	17.85	MIS 2.2
763.5	28	MIS 3.1
939.5	43.88	MIS 3.13
1085.5	50.21	MIS 3.3
1313	58.96	MIS 4.0
1421	64.09	MIS 4.22
1556	71	Toba ash[b]
1601	73.91	MIS 5.0
1661	79.25	MIS 5.1
1797	96.21	MIS 5.31
1865	103.29	MIS 5.33
1949	110.79	MIS 5.4
2097	122.56	MIS 5.51
2133	125.19	MIS 5.53
2197	129.84	MIS 6.0
2321	135.1	MIS 6.2

MIS represents oxygen isotope events correlated to SPECMAP. Ages are from Martinson et al. (1987) except for MIS 3.1, which is from (Grootes et al., 1993).
[a] All calibrated to calendar years, data from Lee et al. (1999).
[b] Data from Lee et al. (1999).

Core MD97-2151 and about 0.18‰ in Core SO50-31KL occurred from ~14 to ~11 ka during Termination I. The positive $\delta^{13}C$ excursion from ~130 to ~126 ka during Termination II in Core MD97-2151 is even larger, with amplitude of about 0.25~0.40‰. Such stepwise increases in $\delta^{13}C$ resemble the Younger Dryas-style events recorded in benthic $\delta^{13}C$ from the tropical Atlantic during Terminations I to IV (Sarnthein and Tiedemann, 1990). Similar events were also detected in high-resolution benthic $\delta^{13}C$ records from the Pacific (Lund and Mix, 1998) and Indian Ocean (Duplessy et al., 1988).

5. Fluctuations of the SCS deep-water

In general, deep-water $\delta^{13}C$ variations in glacial–interglacial time scale are controlled by changes in the global organic carbon inventory and oceanic deep-water circulation (Shackleton, 1977; Duplessy et al., 1984). Climatically induced changes in the global organic carbon inventory may result in carbon transfer between oceanic DIC, the terrestrial biomass (Shackleton, 1977) and shelf sediments (Broecker, 1982), which lead to changes in the mean ocean $\delta^{13}C$. Modeling indicates that carbon transfer may account for about two thirds of the $\delta^{13}C$ shift within glacial/interglacial cycles in eastern Pacific, and about one third in north Atlantic, and such significant changes of benthic foraminifer $\delta^{13}C$ are synchronous on global scale (Ku and Luo, 1992). The variation patterns of Cores SO50-31KL and MD97-2151 with increasing $\delta^{13}C$ towards the present are also evident in deep-water $\delta^{13}C$ records from the eastern Pacific (Shackleton et al., 1983; Raymo et al., 1990), easternmost Indian Ocean (Holbourn et al., 2005) and Atlantic (Ruddiman et al., 1989; Sarnthein and Tiedemann, 1990). This increasing trend seems to represent a general pattern for global deep-water, which appear to stem from carbon transfer between different reservoirs (Ku and Luo, 1992). Also, the increase in $\delta^{13}C$ seems to agree with the increasing trend of organic carbon accumulation in the ocean toward the present (Ku and Luo, 1992). In addition to the carbon cycle, changes in deep-water circulation may influence global deep-water $\delta^{13}C$ (Duplessy et al., 1984; Duplessy et al., 1988). Most of the Younger Dryas-style stepwise increases in deep-water $\delta^{13}C$ in the Atlantic is believed to relate to the short term reversal of North Atlantic Deep-Water (NADW) circulation, induced by meltwater during Terminations (Sarnthein and Tiedemann, 1990). The Younger Dryas-style stepwise increases in $\delta^{13}C$ of Cores SO50-31KL and MD97-2151, and in cores from the Indian and Pacific Oceans (Duplessy et al., 1988; Mix et al., 1991; Lund and Mix, 1998) may also relate to changes in global deep-water circulation. Therefore, the $\delta^{13}C$ variations in Cores SO50-31KL and MD97-2151 from the SCS agree with records from other oceans, indicating a response to global deep-water variations.

The sources of the SCS deep-water are the intermediate water mass and the deep-water mass above 2500 m in the west Pacific (Jian and Wang, 1997). Thus, Core V19-27 collected at 1373 m water depth in the east Pacific is representative of the source of the SCS deep-water (Mix et al., 1991; Talley, 1993). The $\delta^{13}C$ in Core V19-27 remains about 0.2‰~0.8‰ higher during the last 150 ka than in Core MD97-2151, and the differences during Stage 4 and Stage 6 is somewhat higher than during interglacials (Fig. 4). The $\delta^{13}C$ difference between the two cores may be attributed to the $\delta^{13}C$ decline in deep-water, as it flows from the source in the west Pacific to the SCS. Despite of this difference, the variation patterns of the two records are similar (Fig. 4).

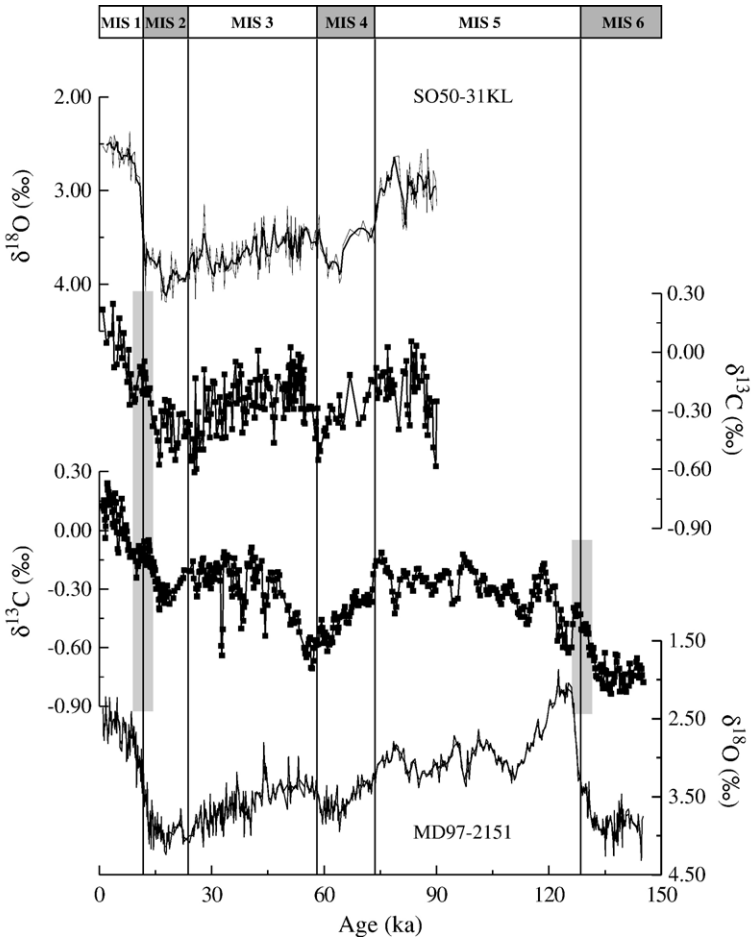

Fig. 3. $\delta^{13}C$ ratios of the benthic foraminifer *C. wuellerstorfi* in Cores MD97-2151 and SO50-31KL. The $\delta^{13}C$ records of Core MD97-2151 were smoothed by a 3-point running average. $\delta^{18}O$ curves were also shown to identify isotope stages. The shaded areas indicate Younger Dryas-style events during Terminations. Horizontal lines indicate the boundaries of oxygen isotope stages.

In order to understand the driving forces behind variations of the SCS deep-water, we performed a spectral analysis on the $\delta^{13}C$ of Core SO50-31KL and MD97-2151 from the SCS, and Core V19-27 from the east Pacific, using the software SPECTRUM (Schulz and Stattegger, 1997). Harmonic analyses (Siegel's Test) of these $\delta^{13}C$ records all exhibit robust Milankovitch cycles (Fig. 5). The 100 ka-eccentricity cycles, 41 ka-obliquity cycles and 23 ka-precession cycles are well expressed in the $\delta^{13}C$ records of Core MD97-2151 and V19-27 within the 6 dB bandwidth. No eccentricity cycle is apparent in the records of Core SO50-31KL due to the short time span, but the obliquity and precession cycles are well expressed (Fig. 5).

In addition to Milankovitch periodicities, high frequency cycle of 8~11 ka is apparent in the $\delta^{13}C$ records of Core SO50-31KL and MD97-2151 with spectral powers above the 95% false alarm levels (Fig. 5). In contrast, Core V19-27 does not exhibit such a periodicity, which may be due to its lower resolution. These high-frequency cycles are probably half-precession cycles that may relate to insolation variations in tropical regions (Berger and Loutre, 1997), and they are also detected in some high-resolution paleoclimate records, such as pollen (Sun et al., 2003; Luo and Sun, 2005; Luo et al., 2005) and TOC contents (Wang, 1999) in the SCS, and paleoproductivity records in the Timor Sea (Holbourn et al., 2005). The power spectrum for TOC in Core MD97-2151 also shows half-precession cycles centering at 9–9.5 ka (Fig. 5). TOC variations are generally related to changes of organic flux from surface water, which is controlled by productivity (Berger et al., 1989), and deep-water $\delta^{13}C$ is significantly influenced by organic matter flux from surface water (Kroopnick, 1985). The half-precession cycles in the SCS deep-water $\delta^{13}C$ therefore suggest that the $\delta^{13}C$ changes in Cores

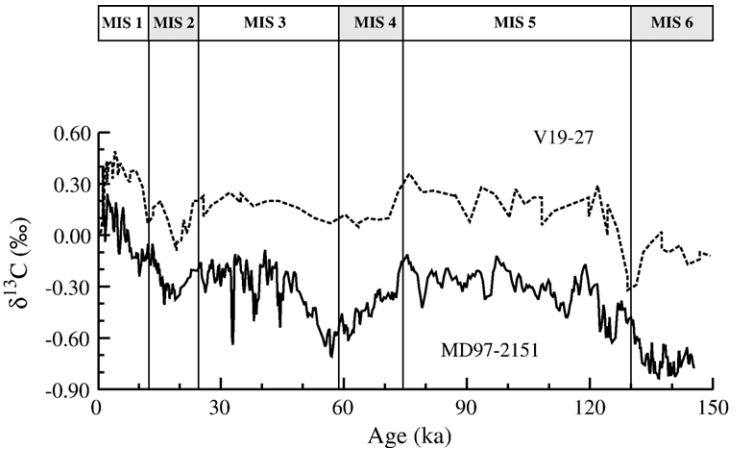

Fig. 4. Comparison of $\delta^{13}C$ records of South China Sea deep water and Pacific intermediate/deep water. Solid lines represent the SCS deep-water records from Core MD97-2151 after smoothing by a 3-point running average. Dashed line represents the Pacific intermediate water record from Core V19-27 (Mix et al., 1991). Horizontal lines indicate the boundaries of oxygen isotope stages.

SO50-31KL and MD97-2151 are partly controlled by surface productivity in the SCS.

In the SCS, surface productivity is heterogeneous and changes during glacial/interglacial cycles (Wang et al., 1999; Jian et al., 2001; Wei et al., 2003). The deep-water in the SCS generally flows from north to south (Wang, 1986), and $\delta^{13}C$ values in the south are generally more negative than in the north (Jian and Wang, 1997; Wang et al., 1999). Recent observations, however, reveal a much complicated pattern for deep water $\delta^{13}C$, which does not always follows deep-water circulation in the SCS (Cheng et al., 2005). Local surface productivity might have a marked effect on the deep-water $\delta^{13}C$ signal in the SCS.

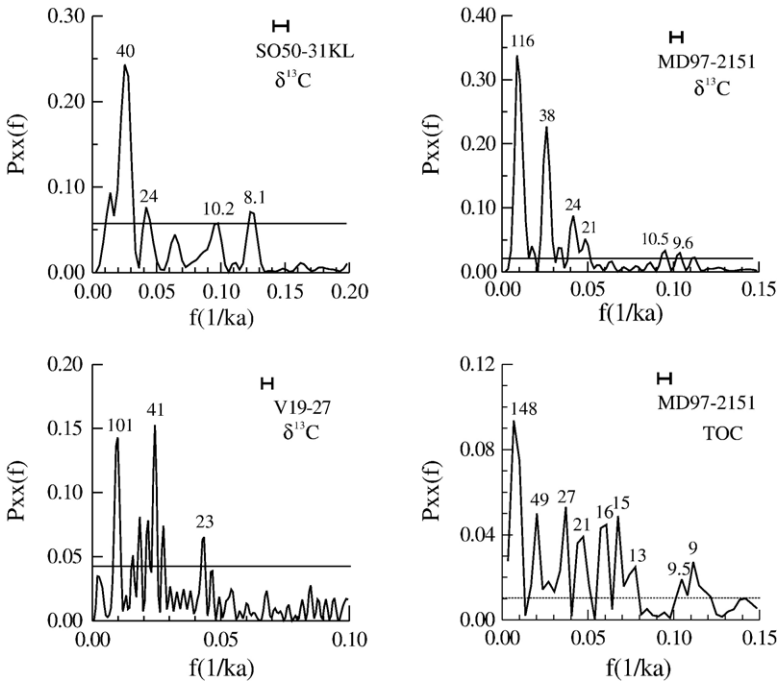

Fig. 5. Harmonic analysis (Siegel's test) of the $\delta^{13}C$ of Cores MD97-2151, SO50-31KL, and V19-27 and TOC contents of Core MD97-2151 using SPECTRUM (Schulz and Stattegger, 1997). Setting: OFAC=4, HIFAC=1, α=0.05, λ=0.4; Horizontal bar marks 6-dB bandwidth, dashed line indicates false alarm level of 95% confidence intervals. Numbers represent the respective frequency of the peaks.

6. Summary

High-resolution $\delta^{13}C$ ratios of the benthic foraminifer, *C. wuellerstorfi* in Core MD97-2151 from the southern SCS and Core SO50-31KL from the northern SCS allow investigating deep-water fluctuations in the SCS during the last 150 ka.

The $\delta^{13}C$ records of these two cores agree well with each other, with higher $\delta^{13}C$ during interglacials than during glacials, increasing $\delta^{13}C$ toward the present, and Younger Dryas-style stepwise increases during Terminations. Such variation patterns agree with global deep-water, implying that variation of the SCS deep-water is generally controlled by global factors, such as carbon cycles and global deep-water circulation. This is further supported by the robust Milankovitch cycles in the SCS deep-water $\delta^{13}C$ records. Whereas significant semi-precession cycles in the spectra of these $\delta^{13}C$ records suggest the influence of local productivity.

Acknowledgement

We thank Dr Chen Y.G. of the Department of Geology, National Taiwan University, for help with the isotope analysis, and Dr Chen M.T. of the National Taiwan Ocean University for valuable advice. Proof reading by Dr. Sun W.D. of Guangzhou Institute of Geochemistry, CAS, helped improve the manuscript. The authors thank Dr A. Holbourn of the Kiel University, Dr. De Lange and an anonymous reviewer for the constructive comments and suggestions. Thanks also go to Dr. Jian Z.M. of the Tongji University for comments on the former version of this manuscript. This study was supported by National Science Council Grants NSC86-2611-M-002-006, NSC86-2611-M-002-04 and NSC88-2119-M-019-002 to C.Y. Huang, and Grant 40173015 of the Natural Science Foundation of China (NSFC) to G.J. Wei.

Appendix A. Supplementary data

Supplementary data associated with this article can be found, in the online version, at doi:10.1016/j.margeo.2006.08.005.

References

Belanger, P.E., Curry, W.B., Matthews, R.K., 1981. Core-top evolution of benthic foraminiferal isotopic ratios for paleo-oceanographic interpretations. Palaeogeogr. Palaeoclimatol. Palaeoecol. 33, 205–220.

Berger, A., Loutre, M.F., 1997. Intertropical latitudes and precessional and half-precessional cycles. Science 278 (5342), 1476–1478.

Berger, W.H., Smetacek, V.S., Wefer, G., 1989. Ocean productivity and paleoproductivity – an overview. In: Berger, W.H. (Ed.), Productivity of the Ocean: Present and Past. John Wiley and Sons, pp. 1–34.

Boyle, E.A., Keigwin, L.D., 1985/86. Comparison of Atlantic and Pacific paleochemical records for the last 215,000 years: changes in deep ocean circulation and chemical inventories. Earth Planet. Sci. Lett. 76, 135–150.

Broecker, W.S., 1982. Ocean chemistry during glacial time. Geochim. Cosmochim. Acta 46, 1689–1705.

Chao, S.Y., Shaw, P.T., Wu, S.Y., 1996. Deep water ventilation in the South China Sea. Deep-Sea Res., Part 1, Oceanogr. Res. Pap. 43 (4), 445–466.

Chen, M.T., Huang, C.Y., 1998. Ice-volume forcing of winter monsoon climate in the South China Sea. Paleoceanography 13 (6), 622–633.

Cheng, X.R., Huang, B.Q., Han, Z.M., Quanhong, Z.H., Tian, J., Li, J.R., 2005. Foraminiferal isotopic evidence for monsoonal activity in the South China Sea: a present–LGM comparison. Mar. Micropaleontol. 54 (1–2), 125–139.

Curry, W.B., Lohmann, G.P., 1982. Carbon isotopic changes in benthic foraminifera from the Western South Atlantic: Reconstruction of glacial abyssal circulation patterns. Quat. Res. 18, 218–235.

Curry, W.B., Duplessy, J.C., Labeyrie, L.D., Shackleton, N.J., 1988. Changes in the distribution of $\delta^{13}C$ of deep water $\sum CO_2$ between the Last Glaciation and Holocene. Paleoceanography 3, 317–341.

Duplessy, J.C., Shackleton, N.J., 1985. Response of global deep-water circulation to the earth's climatic change 135,000–107,000 years ago. Nature 316, 500–507.

Duplessy, J.C., Shackleton, N.J., Matthews, R.K., Prell, W., Ruddiman, W.F., Caralp, M., Hendy, C.H., 1984. ^{13}C record of benthic foraminifera in the Last Interglacial Ocean: implications for the carbon cycle and the global deep water circulation. Quat. Res. 21, 225–243.

Duplessy, J.G., Shackleton, N.J., Fairbanks, R.G., Labeyrie, L., Oppo, D., Kallel, N., 1988. Deepwater source variations during the last climatic cycle and their impact on the global deepwater circulation. Paleoceanography 3, 343–360.

Grootes, P.M., Stuiver, M., White, J.W.C., Johnsen, S., Jouzel, J., 1993. Comparison of Oxygen-Isotope Records from the Gisp2 and Grip Greenland Ice Cores. Nature 366 (6455), 552–554.

Holbourn, A., Kuhnt, W., Kawamura, H., Jian, Z.M., Grootes, P., Erlenkeuser, H., Xu, J., 2005. Orbitally paced paleoproductivity variations in the Timor Sea and Indonesian Throughflow variability during the last 460 kyr. Paleoceanography 20 (3).

Jian, Z.M., Wang, L.J., 1997. Late Quaternary benthic foraminifera and deep-water paleoceanography in the South China Sea. Mar. Micropaleontol. 32 (1–2), 127–154.

Jian, Z.M., Wang, L.J., Kienast, M., Sarnthein, M., Kuhnt, W., Lin, H.L., Wang, P.X., 1999. Benthic foraminiferal paleoceanography of the South China Sea over the last 40,000 years. Mar. Geol. 156 (1–4), 159–186.

Jian, Z.M., Wang, P.X., Chen, M.P., Li, B.H., Zhao, Q.H., Buhring, C., Laj, C., Lin, H.L., Pflaumann, U., Bian, Y.H., Wang, R.J., Cheng, X.R., 2000. Foraminiferal responses to major Pleistocene paleoceanographic changes in the southern South China Sea. Paleoceanography 15 (2), 229–243.

Jian, Z., Huang, B., Kuhnt, W., Lin, H.L., 2001. Late Quaternary upwelling intensity and East Asian monsoon forcing in the South China Sea. Quat. Res. 55 (3), 363–370.

Keigwin, L.D., 1998. Glacial-age hydrography of the far northwest Pacific Ocean. Paleoceanography 13 (4), 323–339.

Kroopnick, P.M., 1985. The distribution of ^{13}C of $\sum CO_2$ in the world oceans. Deep-Sea Res. 32, 57–84.

Ku, T.-L., Luo, S., 1992. Carbon isotopic variations on glacial-to-interglacial time scales in the ocean: modeling and implications. Paleoceanography 7 (5), 543–562.

Lee, M.Y., Wei, K.Y., Chen, Y.G., 1999. High resolution oxygen isotope stratigraphy for the last 150,000 years in the southern South China Sea: Core MD972151. Terr. Atmos. Ocean. Sci. 10 (1), 239–254.

Lund, D.C., Mix, A.C., 1998. Millennial-scale deep water oscillations: reflections of the North Atlantic in the deep Pacific from 10 to 60 ka. Paleoceanography 13 (1), 10–19.

Luo, Y.L., Sun, X.J., 2005. Vegetation evolution and millennial-scale climatic fluctuations since Last Glacial Maximum in pollen record from northern South China Sea. Chin. Sci. Bull. 50 (8), 793–799.

Luo, Y.L., Sun, X.J., Han, Z.M., 2005. Environmental change during the penultimate glacial cycle: a high-resolution pollen record from ODP Site 1144, South China Sea. Mar. Micropaleontol. 54 (1–2), 107–123.

Martinson, D.G., Pisias, N.G., Hays, J.D., Imbrie, J., Moore, T.C., Shackleton, N.J., 1987. Age dating and the orbital theory of the ice ages: development of a high-resolution 0 to 300,000-year chronostratigraphy. Quat. Res. 27, 1–30.

McCorkle, D.C., Keigwin, L.D., 1994. Depth profiles of Delta-C-13 in bottom water and core top C-Wuellerstorfi on the Ontong Java Plateau and Emperor Seamounts. Paleoceanography 9 (2), 197–208.

Miao, Q.M., Thunell, R.C., 1996. Late Pleistocene–Holocene distribution of deep-sea benthic foraminifera in the South China Sea and Sulu Sea: paleoceanographic implications. J. Foraminiferal Res. 26 (1), 9–23.

Mix, A.C., Pisias, N.G., Zahn, R., Rugh, W., Lopez, C., Nelson, K., 1991. Carbon-13 in Pacific deep and intermediate waters, 0–370 ka: implications for ocean circulation and Pleistocene carbon dioxide. Paleoceanography 6 (2), 205–226.

Oppo, D.W., Fairbanks, R.G., 1987. Variability in the deep and intermediate water circulation of the Atlantic Ocean during the past 25,000 years: Northern Hemisphere modulation of the Southern Ocean. Earth Planet. Sci. Lett. 86, 1–15.

Raymo, M.E., Ruddiman, W.F., Shackleton, N.J., Oppo, D.W., 1990. Evolution of Atlantic–Pacific $\delta^{13}C$ gradients over the last 2.5 m.y. Earth Planet. Sci. Lett. 97 (3–4), 353–368.

Ruddiman, W.F., Raymo, M.E., Martinson, D.G., Clemens, B.M., Backman, J., 1989. Pleistocene evolution: Northern Hemisphere ice sheets and North Atlantic Ocean. Paleoceanography 4, 353–412.

Sarnthein, M., Tiedemann, R., 1990. Younger Dryas-style cooling events at glacial Termination I–VI at ODP Site 658: associated benthic $\delta^{13}C$ anomalies constrain meltwater hypothesis. Paleoceanography 5, 1041–1055.

Schulz, M., Stattegger, K., 1997. SPECTRUM: spectral analysis of unevenly spaced paleoclimatic time series. Comput. Geosci. 23 (9), 929–945.

Shackleton, N.J., 1977. Tropical rainforest history and the equatorial Pacific carbonate dissolution cycles. In: Andersen, N.R., Malahoff, A. (Eds.), The Fate of Fossil Fuel CO_2 in the Oceans. Plenum, New York, pp. 401–428.

Shackleton, N.J., Imbrie, J., Hall, M.A., 1983. Oxygen and carbon isotope record of East Pacific core V19-30: implications for the formation of deep water in the late Pleistocene North Atlantic. Earth Planet. Sci. Lett. 65, 233–244.

Sun, X.J., Luo, Y.L., Huang, F., Tian, J., Wang, P.X., 2003. Deep-sea pollen from the South China Sea: Pleistocene indicators of East Asian monsoon. Mar. Geol. 201 (1–3), 97–118.

Talley, L.D., 1993. Distribution and formation of north Pacific intermediate water. J. Phys. Oceanogr. 23 (3), 517–537.

Wang, J., 1986. Observation of abyssal flows in the Northern South China Sea. Acta Oceanogr. Taiwanica 16, 36–45.

Wang, C.C., 1999. High-resolution paleomonsoon/paleoceanography fluctuation of the South China Sea in the last 150 kyrs: records of IMAGES MD972151 core. Dissertation for Master's Degree Thesis, National Taiwan University, Taipei.

Wang, L., Sarnthein, M., Erlenkeuser, H., Grimalt, J., Grootes, P., Heilig, S., Ivanova, E., Kienast, M., Pelejero, C., Pflaumann, U., 1999. East Asian monsoon climate during the Late Pleistocene: high-resolution sediment records from the South China Sea. Mar. Geol. 156 (1–4), 245–284.

Wei, G.J., Liu, Y., Li, X.H., Chen, M.H., Wei, W.C., 2003. High-resolution elemental records from the South China Sea and their paleoproductivity implications. Paleoceanography 18 (2), 1054–1065.

Winn, K., Zheng, L.F., Erlenkeuser, H., Stoffers, P., 1992. Oxygen/carbon isotopes and paleoproductivity in the South China Sea during the past 110 000 years. In: Jin, X.L., Kudrass, H.R., Pautot, G. (Eds.), Marine Geology and Geophysics of the South China Sea. China Ocean Press, Beijing, pp. 154–166.